



Effect of extension of the heparin binding pocket on the structure, stability, and cell proliferation activity of the human acidic fibroblast growth factor



Julie Eberle Davis^a, Ravi Kumar Gundampati^a, Srinivas Jayanthi^a, Joshua Anderson^a, Abigail Pickhardt^a, Bhanu prasanth Koppolu^b, David A. Zaharoff^b, Thallapuram Krishnaswamy Suresh Kumar^{a,*}

^a Department of Chemistry and Biochemistry, University of Arkansas, 1 University of Arkansas, Fayetteville, AR 72701, USA

^b Joint Department of Biomedical Engineering, North Carolina State University and University of North Carolina-Chapel Hill, NC 27695, USA

ARTICLE INFO

Keywords:

Fibroblast growth factor
Heparin binding
Stability
Cell proliferation

ABSTRACT

Acidic human fibroblast growth factor (hFGF1) plays a key role in cell growth and proliferation. Activation of the cell surface FGF receptor is believed to involve the glycosaminoglycan, heparin. However, the exact role of heparin is a subject of considerable debate. In this context, in this study, the correlation between heparin binding affinity and cell proliferation activity of hFGF1 is examined by extending the heparin binding pocket through selective engineering via charge reversal mutations (D82R, D84R and D82R/D84R). Results of biophysical experiments such as intrinsic tryptophan fluorescence and far UV circular dichroism spectroscopy suggest that the gross native structure of hFGF1 is not significantly perturbed by the engineered mutations. However, results of limited trypsin digestion and ANS binding experiments show that the backbone structure of the D82R variant is more flexible than that of the wild type hFGF1. Results of the temperature and urea-induced equilibrium unfolding experiments suggest that the stability of the charge-reversal mutations increases in the presence of heparin. Isothermal titration calorimetry (ITC) data reveal that the heparin binding affinity is significantly increased when the charge on D82 is reversed but not when the negative charge is reversed at both positions D82 and D84 (D82R/D84R). However, despite the increased affinity of D82R for heparin, the cell proliferation activity of the D82R variant is observed to be reduced compared to the wild type hFGF1. The results of this study clearly demonstrate that heparin binding affinity of hFGF1 is not strongly correlated to its cell proliferation activity.

1. Introduction

FGFs are a family of polypeptides involved in a wide range of core signaling processes that govern cell growth, cell proliferation, cell differentiation, stress response and wound healing [1–7]. FGFs exert their action(s) by binding to their cell surface receptors (FGFRs) [1,6–9]. FGF1 is the only member of the FGF family that binds with high affinity to all four types of FGFRs [10,11]. Formation of the hFGF1/FGFR complex, initiates the processes of dimerization and autophosphorylation of the intracellular tyrosine kinase domain, ultimately triggering downstream signaling [12].

hFGF1-receptor interaction is believed to be highly dependent on heparin, a glycosaminoglycan that is commonly found in the extracellular matrix of mammalian cells at concentrations up to 10^6 units per

cell [5,13–15]. Heparin consists of long, unbranched, helical chains of repeating disaccharide units, which are heavily sulfonated [13]. Heparin is also believed to be critical for the biological activity of hFGF1 [16]. Crystal structures of the hFGF1/FGFR complex suggest that heparin directly contacts both hFGF1 and the receptor [16].

Crystal and solution structures of the heparin-FGF complex show that the glycosaminoglycan binds to a cluster of positively charged residues, which are located at the c-terminal end of the molecule. The residues involved in the putative heparin-binding pocket of hFGF1 include K126, K127, K132, R133, R136, and K142 [17]. These heparin-binding amino acids form a region of concentrated positive charge that renders hFGF1, in its unbound form, to be relatively unstable and prone to thermal and proteolytic degradation [4,18–20]. Therefore, hFGF1 binding to heparin increases the stability of the growth factor [8,9].

Abbreviations: hFGF1, human fibroblast growth factor-1; SDM, site directed mutagenesis; CD, circular dichroism; HSQC, heteronuclear single quantum coherence; ATCC, American Type Culture Collection; VMD, Visual Molecular Dynamics; ITC, Isothermal titration calorimetry

* Corresponding author.

E-mail address: sthalla@uark.edu (T.K.S. Kumar).

<https://doi.org/10.1016/j.bbrep.2017.12.001>

Received 22 August 2017; Received in revised form 5 December 2017; Accepted 11 December 2017

Available online 22 December 2017

2405-5808/ © 2017 The Authors. Published by Elsevier B.V. This is an open access article under the CC BY-NC-ND license (<http://creativecommons.org/licenses/by-nc-nd/4.0/>).

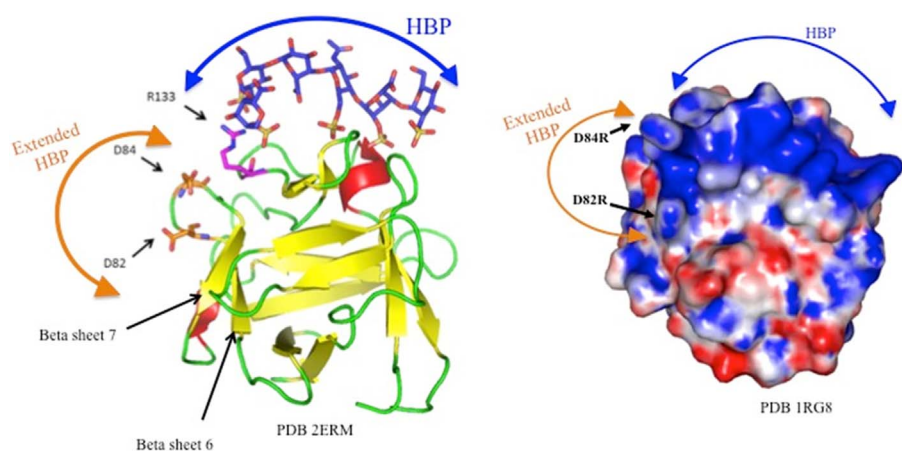


Fig. 1. Left - Three-dimensional structure of hFGF1 (PDB 2ERM) depicting the side-chain of the positively charged residue R133 in the heparin-binding pocket. The heparin-binding pocket has been extended through reversal of charge on D82 (D82R) and D84 (D84R). Right - Representation of the electrostatic potential in the three-dimensional structure of hFGF1 showing that charge reversal(s) at D82 and D84 extends the heparin-binding region of hFGF1 (PDB 1RG8).

Furthermore, heparin's interaction with FGFRs stabilizes the hFGF1-FGFR binary complex [5,16,21,22]. However, there has been a long-standing debate on whether heparin is obligatory for hFGF1 activity. The initial “dogma” describes heparin's role as a mandatory co-receptor that is critical for cell signaling events triggered by hFGF1 [14,16,23,24]. However, there are significant reports to the contrary, which suggest that heparin is only necessary for stabilizing the growth factor [4,12,18,20,25,26]. In this context, the debate on the exact role of heparin in the FGFR signaling process is still an open question.

Several studies using a site-directed mutagenesis approach have identified several conserved residues, which, when appropriately mutated, increased the thermodynamic stability of hFGF1. In addition, several mutant forms of hFGF1 have exhibited mitogenic activity even in the absence of heparin [4,12,18–20,25,26]. One notable mutation is the charge-reversed substitution K132E in the heparin-binding pocket, which was found to reduce hFGF1's affinity for heparin [12]. Interestingly, it has been shown that introduction of thermally stabilizing mutations into hFGF1 variants with reduced affinity for heparin, such as K132E, have been shown to compensate for lack of heparin involvement in FGFR activation [12]. While these studies suggest that heparin binding to hFGF1 is not critical for the protein's mitogenic activity, heparin is still opined to have a critical role in hFGF1 receptor binding and signaling [9,27–29].

One approach to assess the role of heparin that has yet to be investigated is the evaluation of hFGF1 activity using mutations that are predicted to increase heparin binding. In this context, we have studied the correlation between heparin-binding affinity and cell proliferation activity of hFGF1 by designing charge-reversal mutations in the vicinity of the heparin binding pocket involving the substitution of aspartic acid for arginine at position 82 and 84 (PDB 2ERM) [17]. Specifically, D82R and D84R mutations have been designed to extend the heparin-binding interface on hFGF1. Crystal structures of hFGF1, both with and without heparin, were used to measure the distance between the carboxyl side chain group of D82 and the guanidinium side chain group of R133. Comparison of these measurements reveals that the position of D82 in the heparin-bound hFGF1 structure is 6 Å farther away from the heparin-binding region than it is in the native hFGF1 structure. D82N is also included as a control mutant to determine if a lack of negative charge at this position influences the protein's structure, stability, activity, and interaction differently than the D82R mutant.

Results of this study show that charge reversal at position 82 destabilizes hFGF1 structure. Furthermore, although charge reversals D82R and D84R increase heparin-binding affinity, they do not concomitantly increase the cell proliferation activity of hFGF1. The results obtained in this study strongly suggest that heparin merely increases the bioavailability of hFGF1 at the cell surface and thereby enhances the probability of a productive hFGF1-receptor interaction. For this study, all protein samples were derived from expression in *E. coli*, an

expression system that lacks post-translational modification. However, hFGF1 is not known or predicted to undergo post-translational modification that would potentially affect the heparin binding.

2. Results and discussion

Human acidic fibroblast growth factor (hFGF1) is a beta-barrel protein with 12 antiparallel beta-strands. The canonical heparin-binding pocket is located at the c-terminal end between beta strands 10 and 12. Positively charged residues densely populate the heparin-binding pocket in the protein. Site-directed mutagenesis studies have shown that the positively charged residues in the heparin-binding pocket are critical for the heparin binding affinity of hFGF1 [30,31]. In this study, we have used low weight molecular heparin as it is well known that high molecular weight heparin is polydispersed, containing a heterogeneous mixture of heparin molecules of varying chain lengths. The high polydispersity poses significant technical challenge in the interpretation of the NMR results. In addition, in our experience, the high polydispersity also presented serious problems in calculating the average molecular weight, which in-turn adversely influenced the heparin concentration determination(s). The low polydispersity of the low molecular heparin significantly diminished the above-mentioned technical difficulties. Furthermore, the low molecular weight ($M_r \sim 3000$ Da) heparin used has been estimated to be 8–12 units long and multiple studies have shown that heparin with a chain length of 8-units has been shown to be sufficient to facilitate optimal FGF-induced cell signaling [13,32,33].

2.1. Spatial proximity of D82/D84 to the putative heparin-binding pocket

Residues D82 and D84 are located on the protein surface within the linker region connecting beta strands 6 and 7 (Fig. 1). In the folded conformation of hFGF1, both D82 and D84 residues appear to be fully solvent-exposed [17]. Thus, neither amino acid is involved in the inner core network of hydrogen bonding or electrostatic interactions stabilizing the three-dimensional structure of the protein. The side chain carboxyl groups of D82 and D84 are located within a spatial distance of 5 Å from T83, L86, L87, and Y88. Neither D82 nor D84 is a part of the canonical heparin-binding pocket. The position of both D82 and D84 in relation to R133, which is in the midst of the heparin-binding pocket, was measured using crystal structures of native hFGF1 in the presence (PDB 2ERM) and absence of heparin (PDB 1RG8) [17,32]. In the absence of heparin, D82 and D84 are positioned ~ 6.9 Å and ~ 6.1 Å, respectively, away from the critical heparin-binding residue R133 (PDB 1RG8) [32]. In the presence of a hexasaccharide heparin chain (PDB 2ERM), D84 is shifted modestly closer to R133 (~ 5.8 Å) while D82 is measured at ~ 12.8 Å from R133.

Using the crystal structure of hFGF1-heparin-FGFR ternary complex

(PDB 1E00), as well as a structure of the symmetrical hFGF1 dimer bound to a decasaccharide heparin chain (PDB 1AXM), it was determined that D82 of each hFGF1 monomer is within 8 – 11 Å from the sulfate groups of the third unit (D-glucosamine) in the heparin chain [23]. Replacement of aspartic acid with arginine at position 82 (D82R) in both hFGF1 monomers would bring the side chain even closer to the sulfate groups of heparin. It is evident from the crystal structure(s) of both complexes (PDB 1E00 and 1AXM) that the heparin chain must be approximately ten saccharide units long to facilitate the heparin-induced dimerization of hFGF1 [23]. Furthermore, taking in to account the dynamic nature of the molecular interaction(s), the side chain of arginine at position 82 and 84 would be placed within 3–8 Å of the closest sulfate group on heparin. Thus, substitution of D82 and D84 with arginine apparently would result in the extension of the heparin-binding pocket in hFGF1 and consequently can be potentially expected to provide additional points of contacts for the glycosaminoglycan binding.

Brown *et al.* showed that heparin fragments smaller than the octasaccharide cannot facilitate dimerization and are not physiologically relevant. Furthermore, the binding between hFGF1 and heparin is shown to exhibit a positive cooperativity that preferentially forms oligomers instead of 1:1 complexes, thus suggesting that chain lengths longer than the octasaccharide are more pertinent to the biological activity of hFGF1 [13]. In addition, it was demonstrated that a single heparin chain of molecular mass ~16 kDa can bind up to fifteen hFGF1 molecules [13]. In addition, the alpha helical backbone of heparin is shown to undergo conformational change(s) upon binding to hFGF1 [34]. Although heparin is a relatively rigid molecule in solution, it tends to be kinked upon binding to hFGF1 with alterations in the backbone

torsion angles. The kinked backbone structure of heparin is conducive for favorable electrostatic and van der Waals interactions with hFGF1 [13].

2.2. Individual charge reversals induce stabilizing hydrogen bonding

Molecular dynamic simulations were run to further assess the conclusions drawn from fluorescence, trypsin digestion, and equilibrium unfolding experiments. All simulations were completed using the crystal structure of hFGF1 in the absence of heparin (Protein Data Bank code 1RG8). Movies of each simulation are provided in the [Supplementary Material](#). Interdomain distances of the C α backbone atoms were measured as a function of time for each trajectory and root mean square fluctuation (RMSF) for the C α atoms of each mutant were also determined (Fig. 2A and B). The root mean square deviation (RMSD) of mutant D82N and double mutant D82R/D84R are most similar to wt-hFGF1 showing no major jumps or significant fluctuations. RMSD calculations for D84R slowly increase over the course of the trajectory and reach a maximum of 1.4 Å between the 80–90 ns time mark. This maximum for D84R is modestly higher than the RMSD of wt-hFGF1 suggesting an increased level of flexibility. Increased flexibility within the D84R structure is also observed from RMSF calculations specifically for the loop within the heparin-binding region around residue G129 as well as for a solvent exposed loop outside of the heparin-binding region around residue E95 (Fig. 2B).

Interestingly the RMSD calculation for mutant D82R reveals a jump up to 2 Å around the 70 ns time mark, indicating increased flexibility compared to wt-hFGF1 (Fig. 2A). Furthermore, RMSF values for D82R also show increased flexibility compared to wt-hFGF1 among residues

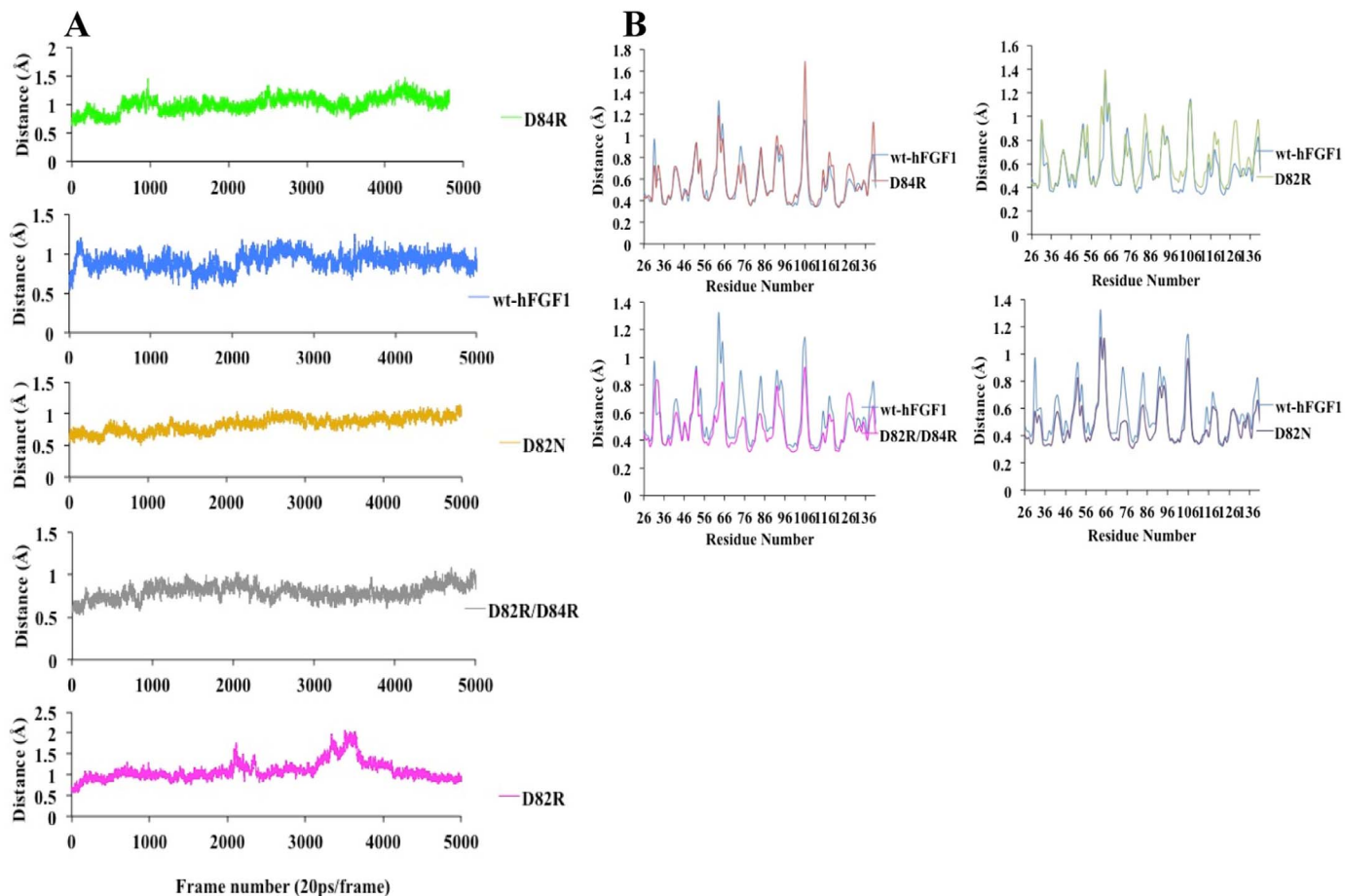


Fig. 2. Panel-A Interdomain distances of the C α backbone atoms as a function of time for each simulation. Panel-B overlay of RMSF values for each designed hFGF1 mutant with wt-hFGF1.

Table 1
Salt bridge analysis for each designed hFGF1 mutant and wt-hFGF1.

| Stable Salt Bridges | | | | | | | | |
|---------------------|---------|---------|---------|----------|----------|----------|-----------|-----------|
| Wt-hFGF1 | D46-R38 | D53-R38 | | | E67-K114 | E95-K115 | E105-K142 | |
| D82R | D46-R38 | D53-R38 | D84-R82 | D84-R133 | E67-K114 | E95-K115 | E105-K142 | |
| D84R | D46-R38 | D53-R38 | D82-R84 | | E67-K114 | E95-K115 | | E118-K119 |
| D82N | D46-R38 | D53-R38 | | | E67-K114 | E95-K115 | E105-K142 | |
| D84R/D82R | D46-R38 | D53-R38 | | | E67-K114 | E95-K115 | E105-K142 | E118-K119 |

in the heparin-binding region (residues V109-G129). This data supports conclusions drawn from fluorescence and trypsin digestion experiments. RMSF calculations for mutant D82N and double mutant D82R/D84R both show overall reduced flexibility among several loop regions outside of the heparin-binding region of the protein. This data along with the RMSD measurements support conclusions drawn from fluorescence and trypsin digestion data that these respective mutations (D82N and D82R/D84R) result in a more compact protein structure.

Salt bridge and hydrogen bonding analysis was also completed for each hFGF1 mutant and wt-hFGF1. Analysis of the D82R trajectory reveals two additional salt bridges that are not present in wt-hFGF1 (Table 1). One salt bridge is formed between the guanidinium head group of R82 and the side chain carboxyl group of D84, which are both on the same loop region between beta strand 6 and 7, and therefore this salt bridge is not an interdomain stabilizing interaction (Fig. 2A, Table 1). The other salt bridge occurs between the side chain carboxyl group of D84 and the guanidinium head group of heparin-binding residue, R133. However, despite the fact that this is an interdomain interaction, it does not increase the stability of the protein in the presence of heat or the chemical denaturant, urea (Fig. 7A, B, Table 2). Similarly, results of the molecular dynamics simulation of the D84R mutant reveal salt bridge formation between the guanidinium head group of R84 and the side chain carboxyl group of D82 (Table 1). Interestingly, these interactions are not present in wt-hFGF1 probably due to repulsion between the closely placed negative charges of D82 and D84.

The molecular dynamics simulation of the D82N mutant indicates that hydrogen bonding occurs between the backbone amide group of N82 and the backbone carbonyl group of L86 but there is also additional hydrogen bonding between the side chain carbonyl group of N82 and the backbone amino group of L86 (See Supplementary Movie). Analysis of salt-bridge formations for the D82N mutant reveals an assessment identical to that of wt-hFGF1 (Table 1). Double charge reversal at combined positions 82 and 84 does not induce the hydrogen bonding that is observed with individual charge reversal mutations (See Supplementary Movie). In fact, analysis of the results of molecular dynamics simulation of the double mutant, D82R/D84R reveal that the guanidinium head groups of R82 and R84 are oriented away from each other. The side chain of R84 appears moderately flexible while R82 is primarily locked into a rigid position due to stabilizing hydrogen bonds formed between the guanidinium head group and the carboxyl side chain of E96 located in the neighboring loop region. Analysis of salt bridge formations for D82R/D84R reveals no significant difference compared to wt-hFGF1 except for the addition of a stable bond between E118 and K119 within the heparin-binding region. Altogether, the

results of molecular simulations indicate that the introduction of positive charge at position 82 increases the flexibility of the protein structure among loops in the heparin-binding region, and does not induce any stabilizing interdomain salt-bridges.

Supplementary material related to this article can be found online at <http://dx.doi.org/10.1016/j.bbrep.2017.12.001>.

2.3. D82R mutation causes a subtle change in the tertiary structure

Wt-hFGF1 and the designed mutant proteins were purified to homogeneity (Fig. S2). D82R, D82N, and D84R mutants exhibit strong binding affinity to heparin and all of them are found to elute in 1500 mM NaCl from the heparin sepharose affinity column. The double mutant, D82RD84R, predominantly eluted in 800 mM NaCl along with some minor bacterial protein impurities and this mutant was subsequently passed over heparin sepharose again to obtain the pure protein (Fig. S2). The yields of the purified wt-hFGF1 and single mutant proteins were in the range of 10–20 mg per liter of bacterial culture. D82RD84R was obtained at reduced yields of 3–5 mg per liter of bacterial culture.

Far UV circular dichroism is a useful technique to obtain reliable information on the secondary structure of proteins [35]. Comparison of the far-UV CD spectra of the hFGF1 mutants (D82R, D82N, and D84R) reveals that they superimpose well with wt-hFGF1 suggesting that the backbone of the protein is folded into the native beta-barrel structure and is not significantly perturbed due to substitution of the negative charge on D82 or D84 with positive charge (Fig. 3). The far-UV CD spectra of the double mutant D82RD84R, with and without heparin, yields the least pronounced positive band from 240 to 220 nm as the wt-hFGF1 does, however the overall spectra of the mutant spectrum indicates that beta barrel structure is not significantly perturbed (Fig. 3).

hFGF-1 contains a lone tryptophan residue at position 121. The intrinsic fluorescence of the lone tryptophan is significantly quenched by the lysine and proline residues, which are located at close spatial proximity to the indole ring [36]. As a consequence, wt-hFGF-1 in its native conformation shows an emission maximum at 308 nm corresponding to the eight tyrosine residues in the protein. However, the quenching effects on the indole ring of Trp121 are completely relieved in the denatured state(s) of the protein and wt-hFGF1 shows the characteristic tryptophan emission peak at 350 nm. Intrinsic fluorescence spectra of wt-hFGF1 and all hFGF1 mutants in the presence and absence of heparin show a maximum emission at 308 nm, a characteristic feature of the native conformation of the protein (Fig. 4). However, the

Table 2
Thermodynamic stability of wt-hFGF1 and the designed mutants.

| Protein | T_m °C | | | C_M (M) | | |
|----------|---------------|---------------|--------------|---------------|--------------|--------------|
| | No heparin | With heparin | ΔT_m | No heparin | With heparin | ΔC_M |
| Wt-hFGF1 | 48.5 (± 0.72) | 68.7 (± 0.68) | 20.2 | 1.8 (± 0.11) | 4.2 (± 0.09) | 2.4 |
| D82R | 45.4 (± 0.59) | 64.3 (± 1.40) | 18.9 | 1.3 (± 0.14) | 4.4 (± 0.02) | 2.8 |
| D84R | 42 (± 0.96) | 71.6 (± 0.51) | 29.6 | 1.62 (± 0.20) | 4.3 (± 0.08) | 2.68 |
| D82N | 49.3 (± 0.72) | 67.0 (± 1.12) | 17.7 | 2.24 (± 0.08) | 4.2 (± 0.04) | 1.96 |
| D82RD84R | 52.6 (± 0.24) | 65.9 (± 0.60) | 13.3 | | | |

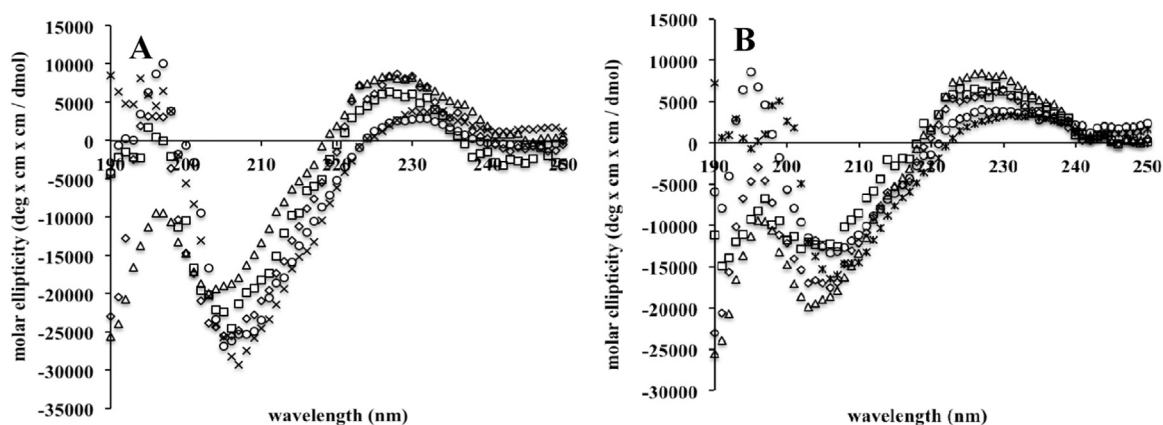


Fig. 3. The Far-UV CD spectra of wt-hFGF1 and the engineered charge reversal mutations in the absence (Panel-A) and presence of heparin (Panel-B). wt-hFGF1 (Δ), D84R (\emptyset), D82R (\circ), D82N (\square), D82R/D84R (\times).

fluorescence spectra of D82R and the double mutant (D82RD84R) show a small hump at 350 nm in addition to the emission maximum at 308 nm. These spectral features suggest that a subtle perturbation of the tertiary structure occurs due to these mutations.

Anilino naphthalene 8-sulfonate (ANS) is a non-polar dye that is commonly used to assess the presence of solvent-exposed hydrophobic surface(s) in proteins. ANS, when bound to wt-hFGF1, and the designed mutants, shows an emission maximum of 520 nm. Comparison of the ANS saturation curves reveals that the relative fluorescence intensity for D84R and D82N mutants is lower than that of wt-hFGF1 (Fig. 5A,B). These results indicate that the charge-reversal at position 84, and the loss of charge mutation at position 82 (D82N) only induce marginal changes in the solvent-exposed hydrophobic surface(s) of the protein. The observed decrease in ANS emission intensity suggests that the structure of the D84R mutant of hFGF1 appears to become more compact upon binding to heparin and consequently the solvent accessibility of the non-polar surface(s) in the protein decreases (Fig. 5). Interestingly, the emission intensity of ANS upon binding to the D82R and D82RD84R mutants, both in the presence and absence of heparin, is about two-fold higher than that observed for the wild type under similar conditions (Fig. 5A,B). These results indicate that charge-reversal at position 82 causes a subtle conformational change resulting in the increased solvent-exposure of non-polar surfaces in the protein. These observations pertaining to the tertiary structure(s) of the D82R and D82RD84R mutants corroborate well with the conclusions drawn from the intrinsic tryptophan fluorescence data.

Limited trypsin digestion is a commonly used method for probing the flexibility of proteins and provides low-resolution information of

structural changes (Fig. 6 and Fig. S3). D82R is quickly degraded by trypsin (85% of the protein is digested in 10 min). After 40 min of incubation with trypsin at 37 °C, the 16 kDa band corresponding to D82R is completely digested. In comparison, at the 40-min time point, wt-hFGF1, D82N and D84R are digested to 15%, 30% and 50%, respectively. Further, D82RD84R mutant of hFGF1 is digested to 25% after 40 min of exposure to trypsin (Fig. 6A). The results of the limited trypsin digestion experiments suggest that the backbone of the D82R mutant, in the absence of heparin, is significantly more flexible than wt-hFGF1 and the D84R mutant. The observed increase in trypsin susceptibility of the D82R mutant is unlikely due to incorporation of an additional trypsin cleavage site in the protein because both D84R and the double mutant (D82RD84R) exhibit lower susceptibility to trypsin action despite containing additional trypsin cleavage site(s). In the presence of heparin, D82R, D84R, and D82RD84R mutants are strongly resistant to limited trypsin digestion (Fig. 6B). Even after 40 min exposure to trypsin, these three mutants remain completely undigested. These results suggest that the charge reversal indeed increases the heparin binding of hFGF1. The observations regarding the flexibility of the hFGF1 mutants, particularly the increase in structural flexibility of the D82R mutant, are consistent with the conclusions drawn from both the intrinsic fluorescence and ANS binding data.

2.4. Heparin effectively increases stability of charge-reversal hFGF1 mutants

Thermal denaturation of hFGF1 was monitored by far-UV CD and the T_m values [temperature wherein which 50% of the protein

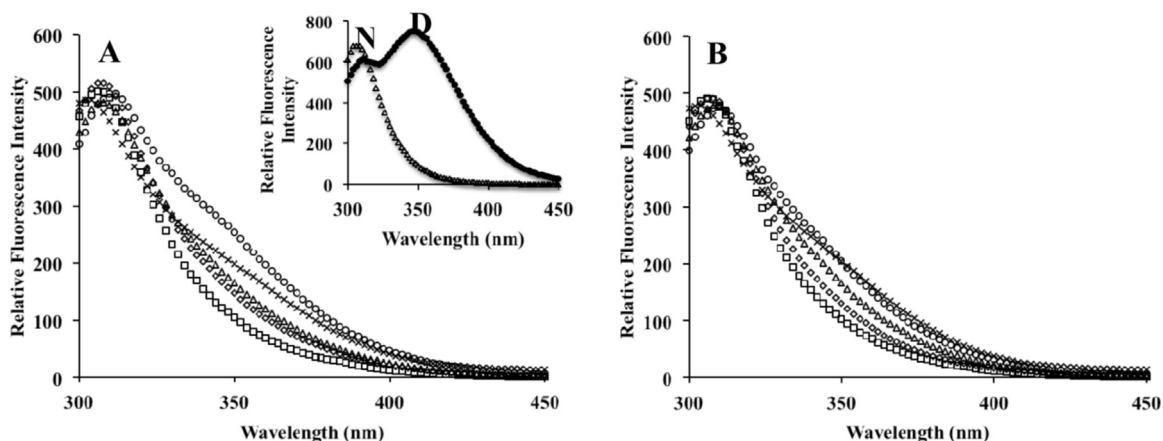


Fig. 4. Intrinsic fluorescence spectra of wt-hFGF1 and the charge-reversal mutants in the absence (Panel-A) and in the presence (Panel-B) of heparin. wt-hFGF1 (Δ), D84R (\emptyset), D82R (\circ), D82N (\square), D82R/D84R (\times). Inset figure in panel A depicts the fluorescence spectra of native (N) and denatured (D) wt-hFGF1.

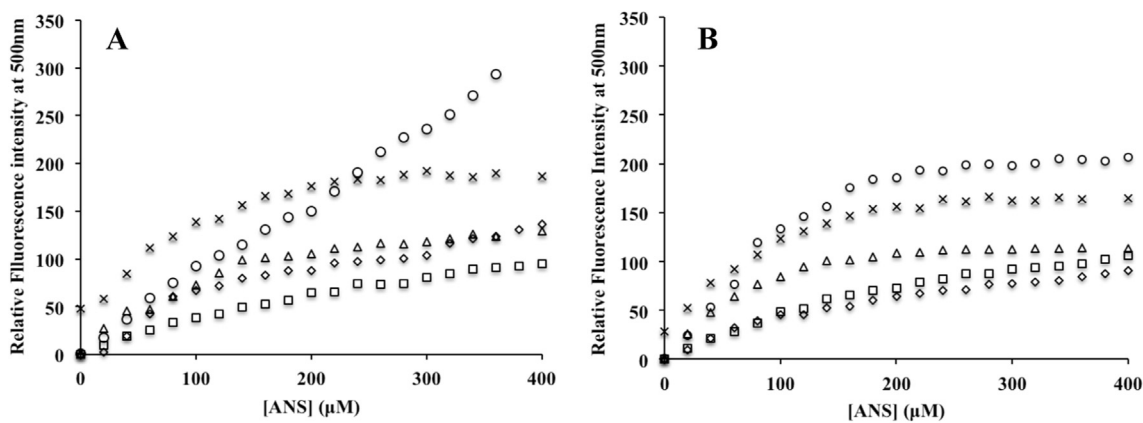


Fig. 5. ANS binding curves of the wild type and the charge reversal mutations of hFGF1 in the absence (Panel-A) and presence (Panel-B) of heparin. Wt-hFGF1 (Δ), D84R (\diamond), D82R (\circ), D82N (\square), D82R/D84R (\times).

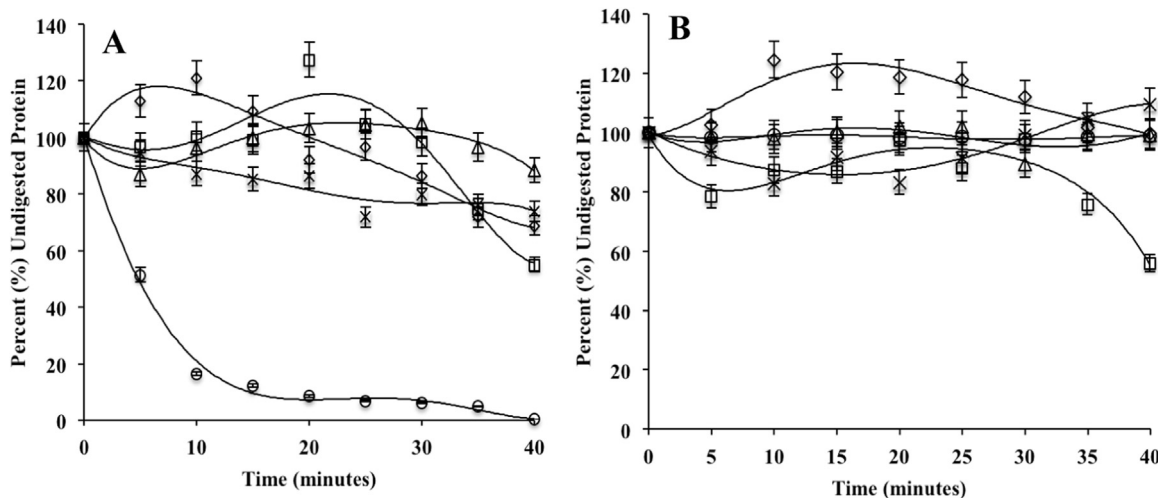


Fig. 6. Densitometric analysis of the section of the SDS PAGE gel depicting the resistance of wild type and charge reversal mutants of hFGF1 to limited trypsin digestion in the absence (Panel-A) and presence (Panel-B) of heparin. Wt-hFGF1 (Δ), D84R (\diamond), D82R (\circ), D82N (\square), D82R/D84R (\times).

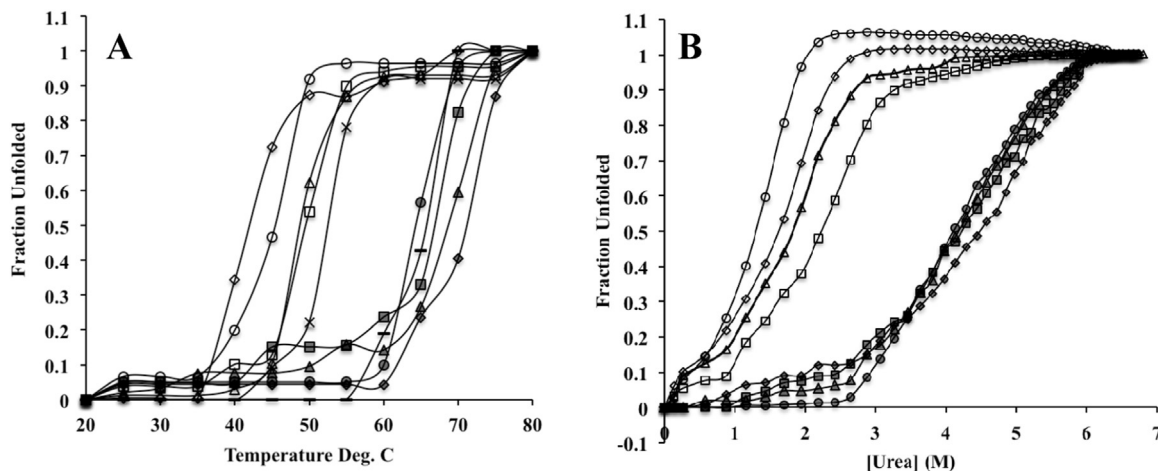


Fig. 7. Thermal (Panel-A) and urea-induced (Panel-B) equilibrium unfolding curves of wild type and the designed mutants of hFGF1 in the presence and absence of heparin. The unfolding curves were monitored by changes in the ratio of the intrinsic fluorescence intensity at 308 nm/350 nm. Absence of heparin: wt-hFGF1 (Δ), D84R (\diamond), D82R (\circ), D82N (\square), D82R/D84R (\times). Presence of heparin: wt-hFGF1 (\blacktriangle), D84R (\blacklozenge), D82R (\blackcirc), D82R/D84R (\blacktimes).

population exists in the denatured state(s)] were calculated from the thermal unfolding curves (Fig. 7A, Table 2). The thermal stability data reveal that, in the absence of heparin, both D82R ($T_m = 45^\circ\text{C} \pm 0.59$) and D84R ($T_m = 42^\circ\text{C} \pm 0.96$) are modestly less stable than wt-hFGF1 ($T_m = 48^\circ\text{C} \pm 0.72$) (Table 1). In contrast, the stability of D82N ($T_m =$

$49^\circ\text{C} \pm 0.72$) remains similar to that of wt-hFGF1. Interestingly, D82RD84R ($T_m = 53^\circ\text{C} \pm 0.24$) is about 4°C more stable than wt-hFGF1 (Table 2). The thermal stability of wt-hFGF1 and the designed charge-reversal mutants effectively increases in the presence of heparin. The thermal stability of heparin-bound D84R ($T_m = 72^\circ\text{C} \pm 0.51$) is

approximately 3 °C higher than that of wt-hFGF1 ($T_m = 69\text{ °C} \pm 0.68$) (Table 2). The total change in thermal stability for D84R due to heparin binding ($\Delta T_m = 30\text{ °C}$) is 10 °C higher than that observed for wt-hFGF1 ($\Delta T_m = 20\text{ °C}$) in the presence of heparin. The T_m for the D82R-heparin binary complex is about 5 °C lower than the melting temperature for wt-hFGF1. The total increase in thermal stability of D82R ($\Delta T_m = 19\text{ °C}$) upon binding to heparin is in the similar range as observed for wt-hFGF1 (Table 2). Furthermore, the large increase in thermal stability observed for D84R agrees well with ANS binding and limited trypsin digestion data demonstrating that heparin binding causes a conformational change in D84R that renders the protein molecule more compact and resistant to trypsin cleavage.

The T_m values for D82N and D82RD84R bound to heparin are 2 °C to 3 °C lower than the T_m measured for wt-hFGF1 in the presence of heparin. Overall, the ΔT_m for D82N ($\Delta T_m = 18\text{ °C} \pm 0.72$) is very similar to the ΔT_m measured for wt-hFGF1 and the ΔT_m for D82RD84R ($\Delta T_m = 13\text{ °C} \pm 0.72$) (Table 2) is approximately 8 degrees lower than wt-hFGF1. The diminished ΔT_m for D82RD84R suggests that heparin binding does not increase its thermal stability as effectively as it does for both the single mutants (D82R and D84R). The discrepancy in the ΔT_m value for the double mutant may be due to possible repulsion generated between the guanidinium head groups at positions 82 and 84. The molecular dynamic simulation data of the double mutant suggested that the R82 and R84 side chains are oriented away from each other to minimize charge-charge repulsion. The altered orientation of the side chains may induce a conformational change that diminishes any contact between heparin and the side chains at position 82 and 84. This inference, pertaining to the D82RD84R mutant, is in good agreement with the conclusions drawn from the far-UV CD, intrinsic fluorescence, and the ANS saturation data, which indicate that introduction of two positive charges at positions 82 and 84 perturb the secondary and tertiary structure of the protein and consequently render the hydrophobic surface(s) in the protein to be more solvent-exposed.

The stability of wt-hFGF1 and each hFGF1 mutant was examined using urea-induced equilibrium unfolding (Fig. 7B, Table 2). In the absence of heparin, the C_m values [the concentration of urea at which 50% of the protein population is denatured] for both D82R ($C_m = 1.3\text{ M} \pm 0.14$) and D84R ($C_m = 1.6\text{ M} \pm 0.2$) are similar to wt-hFGF1 ($C_m = 1.8\text{ M} \pm 0.11$) (Table 2), which indicates that these charge-reversal mutations do not significantly alter the stability of the protein. On the other hand, the C_m of D82N ($C_m = 2.2\text{ M} \pm 0.08$) (Table 2) was observed to be about 0.4 M higher than that of wt-hFGF1. This indicates that loss of charge at position 82 slightly increases the stability of the

protein in the presence of urea. Once again in the presence of heparin, D82R ($C_m = 4.4\text{ M} \pm 0.02$) and D84R ($C_m = 4.3\text{ M} \pm 0.08$) are as stable as wt-hFGF1 ($C_m = 4.2\text{ M} \pm 0.09$) (Table 2). These results confirm that the charge reversals at positions 82 and 84 do not significantly alter the stability of the protein. Furthermore, the stability ($C_m = 4.2\text{ M} \pm 0.04$) conferred by the binding of heparin to the D82N mutant is similar to that observed for wt-hFGF1 bound to heparin. Overall, the ΔT_m and ΔC_m values determined for D82R, D84R, and D82N suggest that heparin effectively stabilizes these mutants to the same degree as that of wt-hFGF1.

2.5. Increase in heparin-binding affinity of hFGF1 mutants

ITC is an extremely valuable tool for measuring the binding between two interacting molecules. The K_d value measured here for the interaction between heparin and wt-hFGF1 ($K_d = 1.7\text{ }\mu\text{M}$) is comparable to the one reported by Brown and coworkers (Fig. 8) [13]. Identical K_d values are observed for the interaction of heparin with hFGF1 mutants D84R and D82N ($K_d = 1.28\text{ }\mu\text{M}$), and this value is not significantly different from that obtained for wt-hFGF1 (Fig. S4). Interestingly, the K_d value for the interaction of heparin with hFGF1 mutant, D82R, ($K_d = 0.17\text{ }\mu\text{M}$) is approximately one log-fold lower than that exhibited by wt-hFGF1 (Fig. 8). This is expected because introduction of positive charge on the protein surface in proximity to the heparin-binding pocket can be predicted to increase the protein affinity to bind to heparin. The higher binding affinity of the D82R mutant for heparin does not appear to result in a concomitant increase in the thermodynamic stability of the mutant as evidenced by the results of the equilibrium unfolding experiments (Table 2). This may be attributed to the inherent lower stability of the D82R mutant. Comparison of the ΔT_m values (Table 2) indicate that heparin is able to stabilize the D82R mutant and the wild type protein to similar extent(s). The K_d values for both D84R and D82N indicate only a modest increase in affinity for heparin compared to wt-hFGF1 (Fig. 8). In contrast, the heparin binding affinity for the double mutant D82RD84R is reduced ($K_d = 3\text{ }\mu\text{M}$) compared to wt-hFGF1 indicating that the behavior of the individual charge reversal mutants is not additive.

ITC measurements can also provide valuable information on the thermodynamics of interactions between molecules. The interactions between heparin and hFGF1 that contribute to the enthalpy term include electrostatic interactions, van der Waals forces, and hydrogen bonding. Interactions contributing to the entropic value include conformational changes as well as solvation changes accompanying hFGF1-

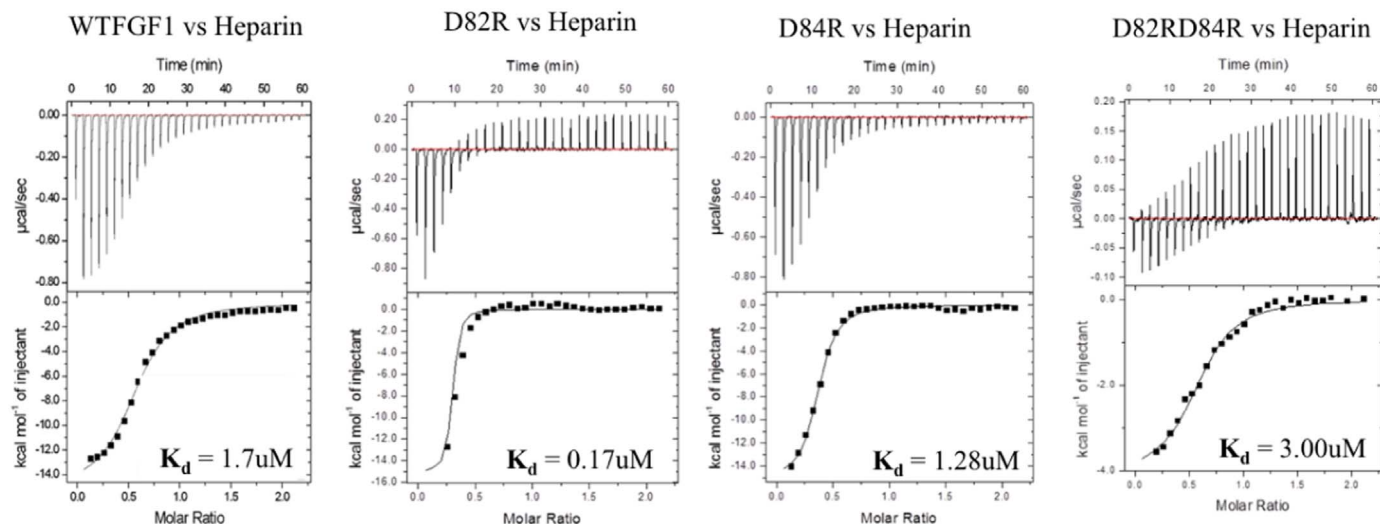


Fig. 8. Isothermograms representing the titration of wild type and the designed mutants with heparin. The upper panels represent the raw heat changes that accompany the binding of the protein to heparin. The lower panels represent the best-fit of the binding curve(s) to a one-site binding model. All ITC data have been corrected for heats of dilution.

Table 3
Thermodynamics of the heparin - hFGF1 interaction.

| Protein | ΔH (kcal/mol) | $-\Delta S$ (kcal/mol) |
|----------|-----------------------|------------------------|
| Wt-hFGF1 | -2.14 ± 0.4 | -1.1 |
| D82R | -3.91 ± 0.1 | -0.5 |
| D84R | -1.6 ± 0.32 | -0.6 |
| D82N | -2.04 ± 0.2 | -1 |
| D82RD84R | -4.1 ± 0.2 | 0.3 |

heparin interaction [13]. For all hFGF1 mutations, the enthalpy value is negative, which indicates favorable binding of hFGF1 to heparin (Table 3). The change in enthalpy associated with D82R-heparin binding ($\Delta H = -1.5 \pm 2.4$ kcal mol⁻¹) is modestly lower than that observed for the wt-hFGF1-heparin binding ($\Delta H = -2.14 \pm 0.4$ kcal mol⁻¹) (Table 3). The change in enthalpy value characterizing the D84R-heparin interaction ($\Delta H = -1.6 \pm 0.32$ kcal mol⁻¹) is also modestly lower than that observed for the wt-hFGF1-heparin interaction, which suggests the degree of contact between this mutant and heparin is marginally reduced.

The change in entropy value for the D82R-heparin interaction ($\Delta S = -0.5$ kcal mol⁻¹) is lower than that for wt-hFGF1-heparin interaction ($\Delta S = -1.1$ kcal mol⁻¹) (Table 3), but is still favorable to promote interaction(s). The lower change in entropy value is likely due to the desolvation occurring at the hFGF1-heparin binding interface. The change in enthalpy value for the D84R-heparin interaction ($\Delta H = -1.6 \pm 0.32$ kcal mol⁻¹) is modestly lower than that of wt-hFGF1-heparin binding. A lower enthalpy value for this mutant may be due to a conformational change, which increases compactness of the tertiary structure.

The thermodynamic values for D82N-heparin interaction ($\Delta H = -2.04 \pm 0.2$ kcal mol⁻¹, $\Delta S = -1$ Kcal mol⁻¹) (Table 3) closely correspond to the values determined for wt-hFGF1-heparin binding. Lastly, the change in enthalpy value accompanying D82RD84R-heparin interaction ($\Delta H = -4.1 \pm 0.2$ Kcal mol⁻¹) is larger than that observed for the wt-hFGF1-heparin interaction, which appears to suggest greater degree of contact between this mutant and heparin. However, the change in entropy value determined for D82RD84R-heparin binding

($\Delta S = 0.3$ kcal mol⁻¹) (Table 3) is unfavorable.

The drastic increase in heparin binding affinity observed for the D82R mutant but not for the D82N is likely due to the presence of the additional positive charge and not due to the neutralization of the negative charge at this position (D82). The lack of drastic increase in affinity of D84R for heparin could be due to local repulsion with the closely placed R133 (PDB 2ERM) [37]. R82 is positioned farther (12.5 Å) away from the canonical heparin-binding residue R133. As the side chain of R82 is positioned on the surface of the protein, the D82R mutation extends the range of positive charge and therefore might accommodate longer heparin chains that span this distance more favorably than the D84R mutant.

2.6. Charge reversal does not significantly perturb the structure of hFGF1

¹H ¹⁵N HSQC is a versatile two-dimensional NMR experiment routinely used to obtain structural information at the individual amino acid level. The structure of wt-hFGF1 has been solved previously and the complete set of assigned resonances is available [17,38]. The ¹H-¹⁵N chemical shift perturbations, upon addition of heparin, were monitored based on chemical shifts assignments published by our group and others [17,38]. Our results compare well with published assignments and therefore assignments can be considered as accurate. Superimposition of HSQC spectra of wt-hFGF1 and D84R mutant and the D82N mutant reveals modest chemical shift perturbations (Fig. S5A and Fig. S6A). The calculated ¹H-¹⁵N chemical shift perturbations indicate that, in both cases (D84R and D82N), most of the significant perturbation occurs in the spatial region close to the location of the mutation site (Fig. S5B and Fig. S6B). However, calculated chemical shift perturbations of D82R determined from the overlay of HSQC spectra of D82R and wt-hFGF1 reveals that the most significant perturbation occurs not only in residues in proximity to the site of the mutation (D84, G85, G89) but also among several residues in the heparin-binding region (K115, K127, K132, and G134) (Fig. 9A and B).

The effect(s) of heparin on the global structure of D82R is determined from the overlay of the HSQC spectra of D82R in the presence and absence of heparin (Fig. 10A). The ¹H-¹⁵N chemical shift perturbation plot of D82R, in the presence and absence of heparin, reveals significant perturbations throughout the protein sequence both in

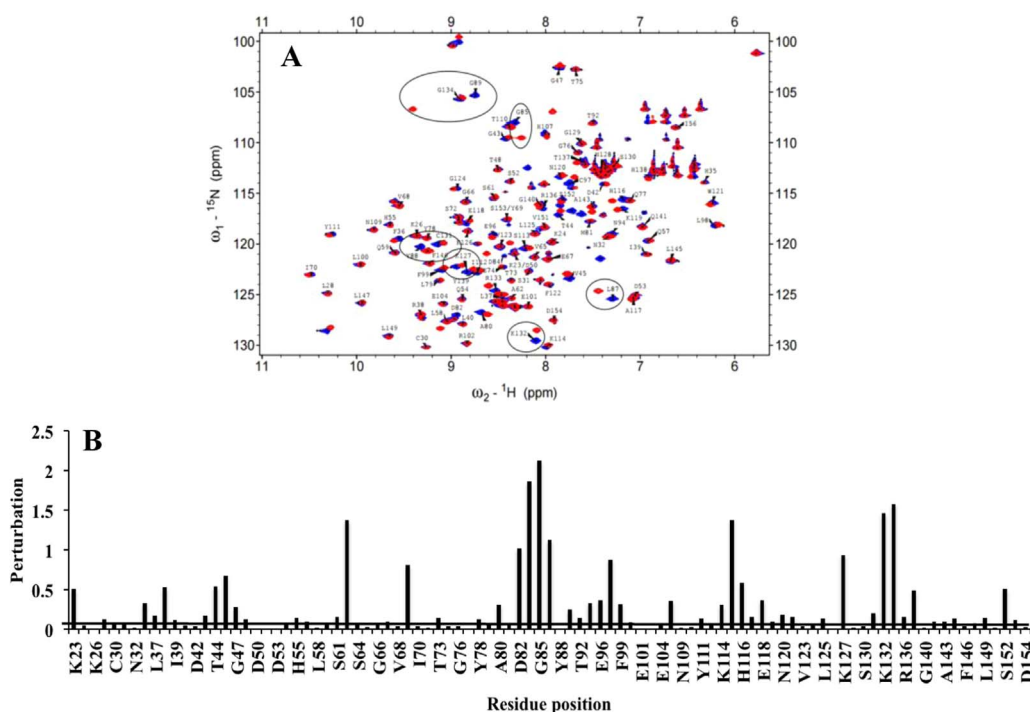


Fig. 9. Panel-A, Overlay of the ¹H-¹⁵N HSQC of wild type (red) and the D82R (blue) mutant of hFGF1. Panel-B, ¹H-¹⁵N chemical shift perturbation observed due to the D82R mutation. The horizontal line represents the arbitrary threshold above which the ¹H-¹⁵N chemical shift perturbation(s) was considered as significant. The ¹H-¹⁵N chemical shift perturbation of individual residues were calculated using the formula, $(\sqrt{[(2\Delta\delta_{NH})^2 + (\Delta\delta_N)^2]})$.

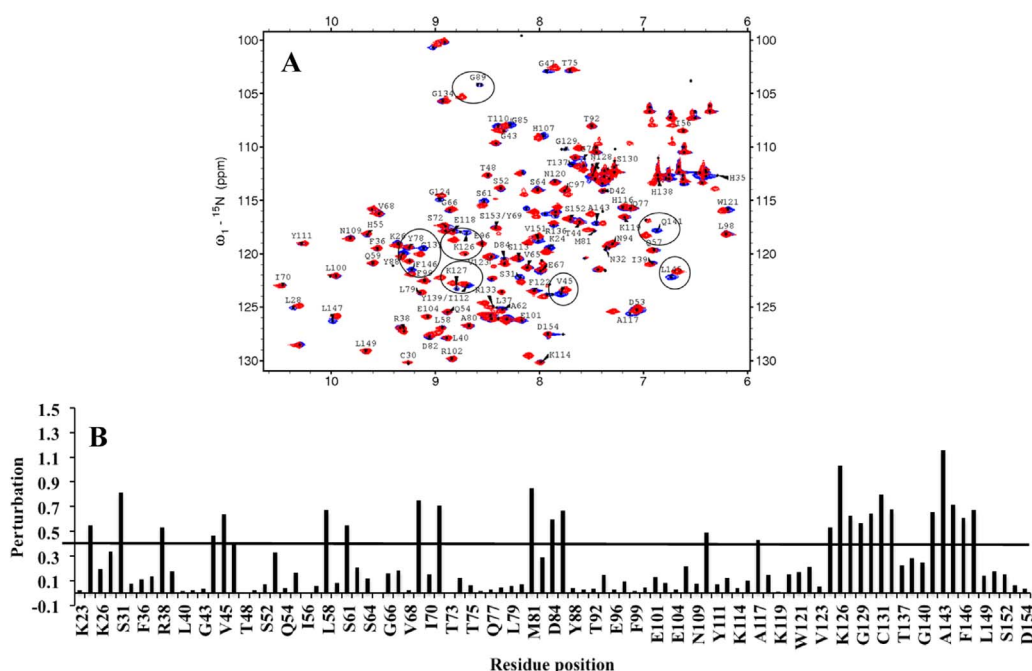


Fig. 10. Panel –A, Overlay of the ¹H–¹⁵N HSQC of D82R mutant of hFGF1 in the presence (blue) and absence of heparin (red). Panel-B, ¹H–¹⁵N chemical shift perturbation observed due to the D82R mutation. The horizontal line represents the arbitrary threshold above which the ¹H–¹⁵N chemical shift perturbation of individual residues were calculated using the formula, $(\sqrt{[(2\Delta\delta_{NH})^2 + (\Delta\delta_N)^2]})$.

proximity to the site of the mutation (M81, D84, G85), and in the heparin-binding region (K126, K127, G129, S130, C131, R136, Q141, A143, L145) (Fig. 10B). These perturbations indicate involvement of these residues in the interaction with heparin.

The heparin binding to the D84R mutation increases the compact nature of the tertiary protein fold, thereby increasing the protein's thermal stability as well as its stability in the presence of the denaturant, urea. However, charge reversal at position 84 does not alter the overall structure of the protein and only marginally increases hFGF1 affinity for heparin. On the other hand, charge reversal at position 82 induces a conformational change that reduces the compact nature of the tertiary fold and increases the protein's flexibility without altering the protein's secondary structure. However, interestingly, charge reversal at position 82 significantly increases hFGF1's affinity for heparin. Loss of charge at position 82 (D82N) seems to have little to no effect on structure, stability, and heparin-binding affinity of hFGF1. While heparin binding to D82N modestly increases the compact character of the protein's tertiary fold. However, no significant changes in stability and

heparin-binding affinity were observed due to this mutation. We could not obtain a quality HSQC spectrum of the double mutant, D82RD84R due to aggregation of the sample during data collection. This aspect precluded us from assessing the change(s) caused in the structure due to the double mutation.

2.7. Increased heparin binding affinity does not correlate with cell proliferation activity

It is believed that heparin is critical for FGF receptor activation. In this context, increased heparin binding affinity of the charged reversed hFGF1 mutants D82R and D84R is expected to result in increased activation of the receptor. The net consequence being increased cell proliferation activity. Cell proliferation study to optimize the heparin: protein ratio was performed on heparinase treated NIH 3T3 cells by varying the concentration of heparin with a fixed concentration of wt-hFGF1 (Fig. S7). Optimum cell proliferation was achieved with a heparin: protein ratio of 10:1. Further cell proliferation experiments were

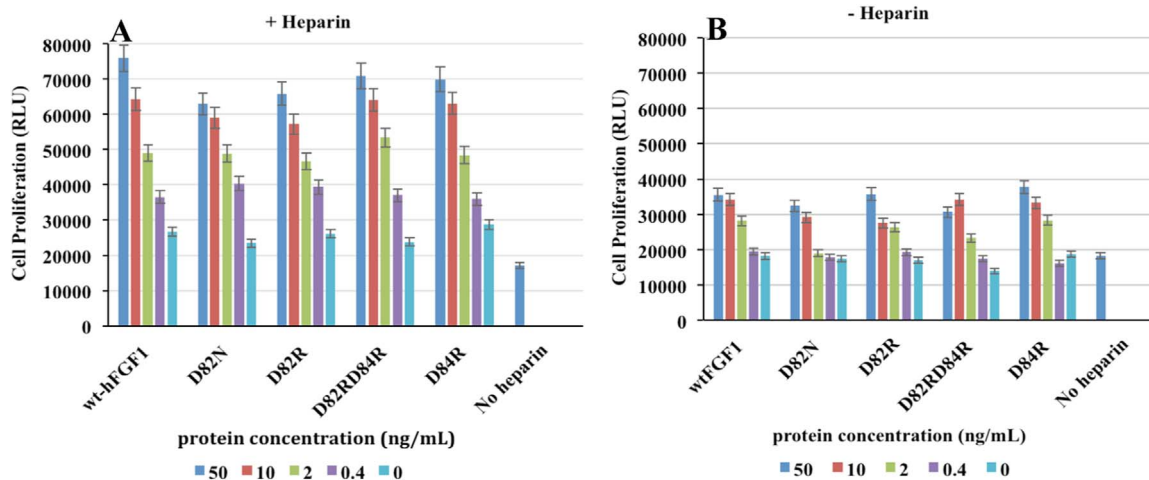


Fig. 11. Panel-A, Proliferation of heparinase treated NIH 3T3 cells in the presence of wild type and the designed mutants of hFGF1 bound to heparin. Panel-B, Proliferation of heparinase treated NIH 3T3 cells in the presence of wild type and the designed mutants of hFGF1 without exogenous heparin. The standard errors were calculated from triplicate measurements (Supplemental Table 1).

then carried out for wt-hFGF1 and each designed hFGF1 mutant using a 10:1 ratio of heparin: protein.

Panel A of Fig. 11 indicates that at the highest protein concentration (50 ng/mL), the level of wt-hFGF1 is not significantly higher than mutant D84R or double mutant D82RD84R, but it does display a statistically higher level of activity compared to single mutants D82R and D82N. Wt-hFGF1 also displays statistically higher cell proliferation activity than D82R at a protein concentration of 10 ng/mL. (No significant statistical differences are observed between wt-hFGF1 and other hFGF1 mutants at protein concentrations below 50 ng/mL) (Fig. 11 Panel-A, Supplemental Table 1). Overall, the cell proliferation data indicate that both mutants (D82R and D84R), despite their increased heparin binding affinity, show similar levels of cell proliferation activity as the wt-hFGF1 in the presence of exogenous heparin (Fig. 11A, Supplemental Table 1). In panel B of Fig. 11, in the absence of exogenous heparin, D82R and D84R are observed to have similar levels of activity as wt-hFGF1 at most all protein concentrations with no statistical differences. D82N and D82RD84R also display similar levels of activity, but D82RD84R is statistically less active than wt-hFGF1 at the highest protein concentration (50 ng/mL) and D82N is statistically less active than wt-hFGF1 at 2 ng/mL. Data produced from bioactivity experiments performed without preliminary heparinase treatment using the same 10:1 heparin: protein ratio yielded the same results as experiments in which heparinase treatment was applied. Altogether, this data again suggests that increased heparin binding does not result in a concomitant increase in the cell proliferation activity of hFGF1.

The notion that heparin's interaction with fibroblast growth factors is not essential for its biological activity has been well documented in the published literature. Two separate groups, Moscatelli and coworkers and Saksela and coworkers, observed that heparin bound human basic FGF (hFGF2) and free hFGF2 interact with its receptor in identical fashion [39]. In another study of hFGF1 mutants, changing two or all three cysteine residues in hFGF1 to serine were shown to have an increased physiological half life and also the biological activity of the mutant proteins was enhanced in a heparin independent manner compared to that of wt-hFGF1 [40]. Wong and coworkers also reported that substitution of K132 to glutamic acid reduces hFGF1 affinity towards heparin, yet they observe full receptor activation as well as early-intermediate gene transcription for the hFGF1 mutant [31]. In addition, several mutagenesis studies have shown that an increase in the thermal stability of hFGF1 confers increased mitogenic activity to the protein in the absence of heparin. Further, L58F and H107S hFGF1 mutations were found to marginally increase the thermal stability by approximately by 3 °C to 7 °C [18,26]. Similarly, Zakrzewska et al. generated several heat stable mutants of hFGF1, which exhibit significantly enhanced heparin-independent cell proliferation activity compared to wt-hFGF1 [4,12,20]. These studies clearly support our conclusions that an increase in heparin binding affinity, through extension of the heparin-binding pocket, does not translate into an increase in the cell proliferation activity of hFGF1. It appears that the primary roles of heparin on the cell surface are: 1.) To enhance the stability of hFGF1 through electrostatic interactions with the densely populated positively charged residues in the heparin binding pocket and 2.) To serve as a reservoir to attract the growth factor molecules to the cell surface and consequently promote FGF-receptor interaction. The results of this study appear to clearly support earlier studies, which suggest that binding of heparin to hFGF1 is not mandatory for its cell proliferation activity.

3. Conclusions

Proteoglycans located on the cell surface help extend the half-life and modulate interaction of many ligands to their corresponding receptors [41]. Particularly, the interaction between hFGF1 and heparin has been studied extensively and overall there are two contrasting views that exist. Initially there has existed a general belief within literature that heparin is critical for binding of hFGF1 to its receptors

[14,23]. This belief was developed from the study of crystal structures of heparin bound hFGF1 dimers in the presence and absence of FGFRs. From these structures, it is observed that the central heparin chain makes contacts with both hFGF1 monomers and one monomer of FGFR. These studies claimed that these ternary complexes are the structural basis for the belief that heparin is essential for hFGF1 signaling and further that hFGF1 dimerization is essential for signaling [23,42]. Recent studies using isothermal titration calorimetry indicate that the oligomerization of hFGF1 to heparin is characterized by positive cooperativity and that an octasaccharide heparin is the shortest length capable of mediating hFGF1 dimerization [13]. However, studies from 2002 and 2005 of monomeric hFGF1 bound to the heparin mimic, *sucrose octasulfate* (SOS), as well as to a synthetic heparin-like hexasaccharide, have found hFGF1 fully capable of FGFR activation and cell proliferation [43,44]. Both studies suggest that oligomerization of the protein is not mandatory for hFGF1 signaling. In this study we were able to show that enhancing the heparin binding property of growth factor hFGF1 through site-directed mutagenesis did not increase the mitogenic activity. This supports the assertion that hFGF1-FGFR interaction for activation of downstream signaling cascades does not critically depend on the binding of either ligand or receptor to the proteoglycan.

4. Materials and methods

4.1. Materials

The Quikchange II XL mutagenesis kit was from Agilent and the DNA plasmid isolation kit was from Qiagen Inc., USA. DH5 α and BL-21(DE3) competent cells were obtained from Novagen Inc., USA. Lysozyme broth is a product of EMD Millipore, USA. Heparin sepharose resin is from GE Healthcare, USA. Buffer components (Na₂HPO₄, NaH₂PO₄, NaCl, and (NH₄)SO₄) were acquired from VWR Scientific., USA. Low molecular weight (~3000 Da) heparin sodium salt was obtained from Sigma and MP Biomedicals LLC. NIH 3T3 cells were obtained from ATCC and all the cell culture reagents including, DMEM media, fetal bovine serum (FBS) and penicillin streptomycin were purchased from Thermo Fisher Scientific (Waltham, MA). All measurements of the spatial distance between residues within hFGF1 were made using Pymol viewing software and were measured as the distance between side chain functional groups (carboxyl groups for D82 and D84, guanidinium group for R133, R82, and R84).

4.2. Molecular dynamic simulations

All mutations were created in Pymol viewing system using the PDB structure 1RG8 [37]. Protein structures were minimized and then solvated with a margin of 10 Å between the protein and the border of the solvent box. The solvent box was neutralized with NaCl at a working concentration of 0.150 M. While hydrogen atoms were kept rigid, the protein backbone, side chains, and solvent molecules/ions were relaxed to prepare the system for equilibration, which was performed in the NPT ensemble utilizing NAMD 2.9 molecular dynamics code and the CHARMM36 force field. First, side chains were minimized for 10,000 steps (each step being 1fs) while the backbone was held rigid in the absence of solvent molecules. Next, with all protein atoms fixed, water molecules were relaxed around the protein over the course of 1500 minimization steps followed by 50 ps of dynamics. A final relaxation step was implemented to relax the solvent molecules around the protein harmonic constraints using a force constant of 1 kcal/(mol Å²). The last operation was the incremental increase of temperature (10 K per 2 ps) to a final temperature of 300 K. Following the temperature increase, the structure was allowed to freely move for 250 ps. Langevin dynamics with a damping coefficient of 1 ps⁻¹ was used to sustain a temperature of 300 K, and Langevin piston method was used to sustain a pressure of 1 atm with a period of 100 fs and a decay time of 50 fs. Long-range

electrostatic interactions were determined using particle mesh Ewald method as well as periodic boundary conditions and a switching function was applied to cut both electrostatic and Van der Waals interactions beyond 12 Å. 100 ns simulations with a time step of 2 fs were performed. Simulations were visualized and hydrogen bonding of the mutated residue was traced in VMD.

4.3. Construction and purification of hFGF1 mutants

A truncated form of hFGF1 (residues, 15–154) was cloned into pET-20b bacterial expression vector was used as a template for site-directed mutagenesis. Primers were designed using an Agilent primer design program and ordered from IDT DNA Inc. Site-directed mutagenesis (SDM) was performed using a QuikChange II XL kit followed by polymerase chain reaction (PCR) as per the protocol provided by the vendor. The plasmid was then transformed into DH5α competent cells. After obtaining confirmation of the plasmid sequences, each mutant protein was overexpressed in BL-21(DE3) *Escherichia coli* cells cultured in lysogeny broth (LB) at 37 °C with agitation of 250 rpm. Overexpressed cells were lysed using ultrasonication (with ~15 W output power) and the desired cell lysate was separated from the cell debris using ultra centrifugation at 19,000 rpm. hFGF1 mutants were then purified on a heparin sepharose column using a stepwise salt gradient in 10 mM sodium phosphate buffer containing 25 mM (NH₄)₂SO₄ pH 7.2 [4,12,20]. The purity of the wt-hFGF1 and the mutant hFGF1 proteins were checked by 15% sodium dodecyl sulfate-polyacrylamide gel electrophoresis (SDS-PAGE) using a prestained protein molecular weight ladder of range 7–175 kDa. Protein bands were visualized by staining the gels with coomassie brilliant blue.

4.4. Isothermal titration calorimetry

The heparin binding affinity of wt-hFGF1 and each mutant were measured using isothermal titration calorimetry (ITC). Protein samples were prepared with 10 mM sodium phosphate buffer containing 100 mM NaCl and 25 mM (NH₄)₂SO₄ pH 7.2. All samples were degassed prior to loading. A 1:10 ratio of protein to ligand (50 μM protein: 500 μM heparin) was applied on a MicroCal iTC200 (Malvern Inc.) in which heparin was titrated into hFGF1 samples. The average molecular mass of heparin used is approximately ~3000 Da, which corresponds to a degree of polymerization anywhere from 8 to 12 saccharides [32]. For each experiment, a series of 30 titrations were performed at 25 °C with a stir speed of 1000 rpm. The data for wt-hFGF1 and the mutants were best-fit to one set of sites and any excess heats of dilution given from heparin were appropriately subtracted out. The binding stoichiometry defined as the maximal number of heparins bound to a hFGF1 molecule can be determined from the inflection point of the titration plot [13].

4.5. Fluorescence spectroscopy and 8-Anilino-1-naphthalenesulfonic acid (ANS) binding

All intrinsic and extrinsic fluorescence measurements were performed on a Hitachi F-2500 spectrophotometer at 25 °C using a slit-width of 2.5 nm and a 10 mm quartz cuvette. Intrinsic fluorescence experiments were performed with protein concentration of 0.1 mg/mL in a 10 mM sodium phosphate buffer containing 100 mM NaCl and 25 mM (NH₄)₂SO₄ (pH 7.2). hFGF1 samples were excited at a wavelength of 280 nm and the emission spectra was recorded from 300 nm to 450 nm. ANS binding assays were performed using a protein concentration of 15 μM. Experiments in the presence of heparin were performed at a heparin to protein ratio of 10:1. Stock ANS was made such that 1 μL titrations into protein sample would increase ANS concentration by 20 μM increments. Fluorescence measurements were made between each titration until saturation was reached. Samples were excited at 380 nm and emission was measured at 520 nm.

4.6. Circular dichroism spectroscopy

Far-UV circular dichroism (Far-UV CD) experiments were performed using a protein concentration of 0.5 μg/μL in 10 mM sodium phosphate buffer containing 10 mM NaCl and 25 mM (NH₄)₂SO₄ (pH 7.2) on a Jasco-1500 spectrophotometer at 25 °C. Experiments performed in the presence of heparin were completed at a heparin to protein ratio of 10:1. For analysis of samples in the presence of heparin, the ligand was added in 10-fold's molar excess of the protein to ensure complete saturation of binding. Necessary background corrections were made and the data was subjected to a smoothing function via application of the Savitzky-Golay algorithm.

4.7. Equilibrium unfolding

Thermal and chemical unfolding of hFGF1 mutants were performed on a Jasco-1500 spectrophotometer through which intrinsic fluorescence and far-UV CD measurements can be made simultaneously. Equilibrium unfolding experiments were performed using a protein concentration of 0.5 mg/mL in 10 mM sodium phosphate buffer containing 10 mM NaCl and 25 mM (NH₄)₂SO₄ at pH 7.2. Experiments including heparin were performed at a heparin to protein ratio of 10:1. Far UV CD data was acquired using a 1 mm quartz cuvette. Spectra were collected every 5 degrees from 20 to 80 °C. Molar ellipticity values were recorded at 228 nm and the fraction unfolded was plotted as a function of temperature. The denaturation temperature (*T_m*) was determined as the temperature at which 50% of the protein population was denatured.

Urea-induced equilibrium unfolding experiments were conducted at a protein concentration of ~0.05 mg/mL. Urea was titrated in consistent volumes into the sample up to a concentration of 6 M. Protein unfolding was monitored by both CD and fluorescence and the fraction unfolded was determined using molar ellipticity values at 228 nm and the ratio of the tyrosine and tryptophan fluorescence (308/350 nm) respectively.

4.8. Limited trypsin digestion

Limited trypsin digestion experiments were performed in the presence and absence of heparin. The initial reaction mixture included 500 μg of protein and 5 μg trypsin in 10 mM sodium phosphate buffer containing 100 mM NaCl, and 25 mM (NH₄)₂SO₄ at pH 7.2. Experiments performed in the presence of heparin were completed with a heparin to protein ratio of 10:1. A second identical sample was prepared with the addition of exogenous heparin in ten times molar excess the protein concentration to ensure saturation of the protein. Trypsin digestion was carried out at 37 °C and a portion of the reaction mixture was removed, at specified time intervals, and the reaction was arrested with the addition of 100% trichloroacetic acid. The reaction products were analyzed by 15% SDS-PAGE and the gels were stained using Coomassie Brilliant Blue (Sigma Aldrich). The percentage of proteolytic digestion was estimated from the band intensity, on the SDS PAGE gel, using UN-SCAN it densitometric software. Intensity of hFGF1 samples not subjected to proteolytic digestion was used as the control representing 100% protection from enzymatic degradation.

4.9. Nuclear magnetic spectroscopy

Heteronuclear single quantum coherence (HSQC) spectroscopy was performed on a Bruker 500 MHz NMR equipped with cryoprobe. The protein samples were isotopically labeled with ¹⁵N as a result of expression in M9 minimal media containing ¹⁵NH₄Cl. All NMR experiments were acquired at 25 °C using a protein concentration of 300 μM using 2 K × 256 data points. Protein samples were prepared in 90% H₂O 10% D₂O solution containing 10 mM sodium phosphate buffer containing 100 mM NaCl and 25 mM (NH₄)₂SO₄ (pH 7.2). The total

chemical shift perturbation per residue ($\Delta\delta_{\text{total}}$) was calculated using the following equation: $\sqrt{[(2\Delta\delta_{\text{NH}})^2 + (\Delta\delta_{\text{N}})^2]}$. All NMR data was analyzed using Sparky 3.114 software [37]. ^1H - ^{15}N chemical shift perturbation at the residue level, caused due to binding of heparin, were carefully tracked by acquiring a series of ^1H - ^{15}N HSQC spectra at different heparin to protein ratio's. Despite our efforts, we could not unambiguously follow the ^1H - ^{15}N chemical shift perturbation of few residues and these residues were not considered in the final ^1H - ^{15}N chemical shift perturbation data presented.

4.10. Cell proliferation assay

3T3 fibroblast cells obtained from ATCC (Manassas, VA) were cultured in complete media consisting of DMEM supplemented with 10% FBS and 1% penicillin/streptomycin. Cells were grown to 80–90% confluency and were incubated overnight at 37 °C with 5% CO_2 in serum free media before further use. Pretreatment of cells with heparinase was performed at a concentration of 6 units of enzyme per 10,000 cells. Cells were incubated with heparinase enzyme for 1 h at 37 °C. Following incubation with heparinase, cells were centrifuged for 2 min at 6000 rpm and then washed twice with hyclone buffer to remove any remaining trace of enzyme and returned to DMEM media with 10% FBS. The cell proliferation activity of hFGF1 was determined by quantifying the increase in cell number after the cells had been incubated with hFGF1 at varying concentrations. Starved 3T3 fibroblasts were collected and seeded in a 96-well plate at a seeding density of 10,000 cells/well. Cells were then co-incubated individually with wild type and mutant hFGF1 at concentrations of 0, 0.4, 2, 10, and 50 ng/mL. The cell proliferation assays were performed in the absence and presence of an optimized 1:10 ratio of hFGF1: heparin. After 24 h of incubation, 3T3 cell proliferation was assessed by the CellTiter-Glo (Promega, Madison, WI) cell proliferation assay.

Acknowledgements

This work was supported by the Department of Energy (grant number DE-FG02-01ER15161), the National Institutes of Health/National Cancer Institute (NIH/NCI) (1 RO1 CA 172631) and the NIH through the COBRE program (P30 GM103450), and the Arkansas Biosciences Institute (ABI-TKSK-2016-17).

Appendix A. Transparency document

Supplementary data associated with this article can be found in the online version at <http://dx.doi.org/10.1016/j.bbrep.2017.12.001>.

Appendix B. Supporting information

Supplementary data associated with this article can be found in the online version at <http://dx.doi.org/10.1016/j.bbrep.2017.12.001>.

References

1. X. Lin, E.M. Buff, N. Perrimon, A.M. Michelson, Heparan sulfate proteoglycans are essential for FGF receptor signaling during *Drosophila* Embryonic Development 126 (1999) 3715–3723.
2. I.J. Mason, The Ins and Outs of Fibroblast growth factors, Cell Press, 1994, pp. 547–552.
3. A.O.M. Wilkie, G.M. Morriss-Kay, E.Y. Jones, J.K. Heath, Functions of fibroblast growth factors and their receptors, Cell Press, 1995, pp. 500–507.
4. M. Zakrzewska, D. Krowarsch, A. Wiedlocha, J. Otlewski, Design of fully active FGF-1 variants with increased stability, Protein Engineering, Design & Selection 17 (8) (2004) 603–611.
5. H. Yu-Peng, et al., Divergent synthesis of 48 heparan sulfate-based disaccharides and probing the specific sugar–fibroblast growth factor 1 interaction, J American Chemical Society (2012) 20722–20727.
6. N. Itoh, D.M. Ornitz, Fibroblast growth factors: from molecular evolution to roles in development, metabolism and disease, J Biochem 149 (2011) 121–130.
7. D.M. Ornitz, N. Itoh, Fibroblast growth factors, Genome Biology 2 (3) (2001) 1–12.
8. E.P. Carter, A.E. Fearon, R.P. Grose, Careless talk costs lives: fibroblast growth factor receptor signalling and the consequences of pathway malfunction, Trends Cell Biol. 25 (4) (2015) 221–233.
9. R. Goetz, M. Mohammadi, Exploring mechanisms of FGF signalling through the lens of structural biology, Nat Rev Mol Cell Biol. 14 (3) (2013) 166–180.
10. D. Miller, S. Ortega, O. Barhayan, C. Basilico, Compensation by fibroblast growth factor 1 (FGF1) does not account for the mild phenotypic defects observed in FGF2 null mice, Mol Cell Biol 20 (2000) 2260–2268.
11. A. Beenken, A.V. Eliseenkova, O.A. Ibrahim, S.K. Olsen, M. Mohammadi, Plasticity in interactions of fibroblast growth factor 1 (FGF1) N terminus with FGF receptors underlies promiscuity of FGF1, J Biol Chem 287 (5) (2012) 30676–33078.
12. M. Zakrzewska, et al., Increased protein stability of FGF1 can compensate for its reduced affinity for heparin, J Biol Chem 284 (37) (2009) 25388–25403.
13. A. Brown, C.J. Robinson, J.T. Gallagher, T.L. Blundell, Cooperative heparin-mediated oligomerization of fibroblast growth factor-1 (FGF1) precedes recruitment of FGFR2 to ternary complexes, Biophys J 104 (2013) 1720–1730.
14. N.J. Harmer, Insights into the role of heparan sulfate in fibroblast growth factor signalling, Biochem Soc Trans 34 (3) (2006) 442–445.
15. M. Hook, L. Kjelle'n, S. Johansson, J. Robinson, Cell-surface glycosaminoglycans, Annu Rev Biochem 53 (1984) 847–869.
16. L. Pellegrini, Role of heparan sulfate in fibroblast growth factor signalling: a structural view, Current Opinion in Structural Biology 11 (2001) 629–634.
17. A. Canales, et al., Solution NMR structure of a human FGF-1 monomer, activated by a hexasaccharide heparin-analogue, FEBS Journal 273 (20) (2006) 4716–4727.
18. J.F. Cula, S.I. Blaber, A. Khyrana, M. Blaber, Thermodynamic characterization of mutants of human fibroblast growth factor 1 with an increased physiological half-life, Biochemistry 39 (24) (2000) 7153–7158.
19. V.K. Dubey, et al., Spackling the crack: stabilizing human fibroblast growth factor-1 by targeting the N and C terminus β -strand interactions, J Mol Biol 371 (2007) 256–268.
20. M. Zakrzewska, D. Krowarsch, A. Wiedlocha, S. Olsnes, J. Otlewski, Highly stable mutants of human fibroblast growth factor-1 exhibit prolonged biological action, J Mol Biol 352 (4) (2005) 860–875.
21. J. Schlessinger, et al., Crystal structure of a ternary FGF–FGFR–heparin complex reveals a dual role for heparin in FGFR binding and dimerization, Mol Cell 6 (2000) 743–750.
22. K. Saxena, et al., Influence of heparin mimetics on assembly of the FGF, J Biol Chem 285 (34) (2010) 26628–26640.
23. L. Pellegrini, D.F. Burke, F. Von Deift, T.L. Blundell, Crystal structure of fibroblast growth factor receptor ectodomain bound to ligand and heparin, Nature 407 (6807) (2000) 1029–1034.
24. J.L. DePaz, et al., The activation of fibroblast growth factors by heparin: Synthesis, structure, and biological activity of heparin-Like oligosaccharides, ChemBioChem 2 (2001) 673–685.
25. A. Szlachcic, et al., Structure of a highly stable mutant of human fibroblast growth factor 1, Acta Cryst D65 (2009) 67–73.
26. S. Brych, S.I. Blaber, T.M. Logan, M. Blaber, Structure and stability effects of mutations designed to increase the primary sequence symmetry within the core region of a β -trefoil, Protein Science 10 (12) (2001) 2587–2599.
27. D.M. Ornitz, N. Itoh, The fibroblast growth factor signaling pathway, Wiley Interdiscip Rev Dev Biol 4 (s) (2015) 215–266.
28. J. Kanodia, F. Greg, Role of HSGAGs in regulation of FGF signaling pathway: insights from mathematical modeling, J Glycobiology 4 (1) (2014), <http://dx.doi.org/10.4172/2168-958X.1000113>.
29. H. Kimura, N. Okubo, N. Chosa, S. Kyakumoto, M. Kamo, H. Miura, A. Ishisaki, EGF positively regulates the proliferation and migration, and negatively regulates the myofibroblast differentiation of periodontal ligament-derived endothelial progenitor cells through MEK/ERK- and JNK Dependent Signals, Cell Physiol Biochem 32 (2013) 899–914.
30. W.H. Burgess, et al., Possible dissociation of the heparin-binding and mitogenic activities of heparin-binding (acidic fibroblast) growth factor-1 from its receptor-binding activities by site-directed mutagenesis of a single lysine residue, J Cell Biol 111 (1990) 2129–2138.
31. P. Wong, B. Hampton, E. Szylobrgt, A.M. Gallagher, M. Jaye, W.H. Burgess, Analysis of putative heparin-binding domains of fibroblast growth factor-1, J Biol Chem 270 (43) (1995) 25805–25811.
32. L. Fu, F. Zhang, G. Li, A. Onishi, U. Bhaskar, P. Sun, R.J. Linhardt, Structure and activity of a new low molecular weight heparin produced by enzymatic ultra-filtration, J Pharm Sci 103 (5) (2014) 1375–1383.
33. C.J. Robinson, N.J. Harmer, S.J. Goodger, T.L. Blundell, J.T. Gallagher, Cooperative dimerization of fibroblast growth factor 1 (FGF1) upon a single heparin saccharide may drive the formation of 2:2:1 FGF1-FGFR2c-heparin ternary complexes, J Biol Chem 280 (51) (2005) 42274–42282.
34. R. Raman, G. Venkataraman, S. Ernst, V. Sasisekharan, R. Sasisekharan, Structural specificity of heparin binding in the fibroblast growth factor family of proteins, PNAS 100 (5) (2002) 2357–2362.
35. A. Micsonai, F. Wien, L. Kernya, Y.H. Lee, Y. Goto, M. Refregiers, J. Kardos, Accurate secondary structure prediction and fold recognition for circular dichroism spectroscopy, PNAS 112 (24) (2015) 3095–3103.
36. P.R. Callis, Binding phenomena and fluorescence quenching. II: photophysics of aromatic residues and dependence of fluorescence spectra on protein conformation, J Mol Structure 1077 (2014) 22–29.
37. M.J. Bennett, T. Somasundaram, M. Blaber, An atomic resolution structure for human fibroblast growth factor 1, Proteins:Structure Function and Bioinformatics 57 (3) (2004) 626–634.
38. Y.H. Chi, et al., Investigation of the structural stability of the human acidic

- fibroblast growth factor by hydrogen-deuterium exchange, *Biochemistry* 41 (51) (2002) 15350–15359.
- [39] D.B. Rifkin, D. Moscatelli, Recent developments in the cell biology of basic fibroblast growth factor, *J Cell Bio* 109 (1989) 1–6.
- [40] S. Ortega, et al., Conversion of cysteine to serine residues alters the activity, stability, and heparin dependence of acidic fibroblast growth factor, *J Biol Chem* 266 (9) (1991) 5842–5846.
- [41] M.A. Nugent, Heparin sequencing brings structure to the function of complex oligosaccharides, *PNAS* 97 (19) (2000) 10301–10303.
- [42] A.D. DiGabriele, I. Lax, D.I. Chen, C.M. Svahn, M. Jaye, J. Schlessinger, W.A. Hendrickson, Structure of a heparin-linked biologically active dimer of fibroblast growth factor, *Nature* 393 (6687) (1998) 812–817.
- [43] A.I. Arunkumar, et al., Oligomerization of acidic fibroblast growth factor is not a prerequisite for its cell proliferation activity, *Protein Science* 11 (5) (2002) 1050–1061.
- [44] J. Angulo, et al., Dynamic properties of biologically activity synthetic heparin-like hexasaccharides, *Glycobiology* 15 (10) (2005) 1008–1015.